PHILOSOPHICAL TRANSACTIONS B

royalsocietypublishing.org/journal/rstb

Research

Cite this article: Edler MK *et al*. 2020 Neuron loss associated with age but not Alzheimer's disease pathology in the chimpanzee brain. *Phil. Trans. R. Soc. B* **375**: 20190619.
http://dx.doi.org/10.1098/rstb.2019.0619

Accepted: 24 March 2020

One contribution of 16 to a theme issue 'Evolution of the primate ageing process'.

Subject Areas:
neuroscience

Keywords:
neuron, glia, brain, chimpanzee, ageing, Alzheimer's disease

Author for correspondence:
Melissa K. Edler
e-mail: medler@kent.edu

Electronic supplementary material is available online at https://doi.org/10.6084/m9.figshare.c.5091150.

THE ROYAL SOCIETY PUBLISHING

Neuron loss associated with age but not Alzheimer's disease pathology in the chimpanzee brain

Melissa K. Edler[1,2,3], Emily L. Munger[1,2,3], Richard S. Meindl[1,2], William D. Hopkins[4], John J. Ely[5], Joseph M. Erwin[6], Elliott J. Mufson[7], Patrick R. Hof[8,9], Chet C. Sherwood[6] and Mary Ann Raghanti[1,2,3]

[1]School of Biomedical Sciences, [2]Department of Anthropology, and [3]Brain Health Research Institute, Kent State University, Kent, OH 44242, USA
[4]Keeling Center for Comparative Medicine and Research, The University of Texas MD Anderson Cancer Center, Houston, TX 77030, USA
[5]MAEBIOS, Alamogordo, NM 88310, USA
[6]Department of Anthropology and Center for the Advanced Study of Human Paleobiology, The George Washington University, Washington, DC 20052, USA
[7]Departments of Neurobiology and Neurology, Barrow Neurological Institute, Phoenix, AZ 85013, USA
[8]Nash Family Department of Neuroscience, Ronald M. Loeb Center for Alzheimer's Disease, and Friedman Brain Institute, Icahn School of Medicine at Mount Sinai, New York, NY 10029, USA
[9]New York Consortium for Evolutionary Primatology, New York, NY 10468, USA

MKE, 0000-0002-9084-9539; ELM, 0000-0001-7437-2032; WDH, 0000-0003-3480-1853; JJE, 0000-0002-2174-3060; EJM, 0000-0003-4438-7334; PRH, 0000-0002-3208-1154; CCS, 0000-0001-6711-449X; MAR, 0000-0002-6842-1907

In the absence of disease, ageing in the human brain is accompanied by mild cognitive dysfunction, gradual volumetric atrophy, a lack of significant cell loss, moderate neuroinflammation, and an increase in the amyloid beta (Aβ) and tau proteins. Conversely, pathologic age-related conditions, particularly Alzheimer's disease (AD), result in extensive neocortical and hippocampal atrophy, neuron death, substantial Aβ plaque and tau-associated neurofibrillary tangle pathologies, glial activation and severe cognitive decline. Humans are considered uniquely susceptible to neurodegenerative disorders, although recent studies have revealed Aβ and tau pathology in non-human primate brains. Here, we investigate the effect of age and AD-like pathology on cell density in a large sample of postmortem chimpanzee brains ($n = 28$, ages 12–62 years). Using a stereologic, unbiased design, we quantified neuron density, glia density and glia:neuron ratio in the dorsolateral prefrontal cortex, middle temporal gyrus, and CA1 and CA3 hippocampal subfields. Ageing was associated with decreased CA1 and CA3 neuron densities, while AD pathologies were not correlated with changes in neuron or glia densities. Differing from cerebral ageing and AD in humans, these data indicate that chimpanzees exhibit regional neuron loss with ageing but appear protected from the severe cell death found in AD.

This article is part of the theme issue 'Evolution of the primate ageing process'.

1. Introduction

As human longevity increases, distinguishing the neurological basis for age-related cognitive decline is imperative. Common cognitive deficits in elderly people include difficulties with complex tasks, word recall, episodic memory and processing speed [1]. Based on magnetic resonance imaging (MRI) studies, these cognitive alterations coincide with decreased brain weight, increased white matter hyperintensity, enlarged lateral ventricles and mild regional volumetric atrophy [2]. Accompanying these gross changes are modest modifications in neurons, dendritic spines, synapses and neurotransmitters along with increased

glial activation, reduced cerebral blood flow and a weakening of the blood-brain barrier [3–5]. Ageing also contributes to an individual's risk for developing Alzheimer's disease (AD), the most prevalent form of dementia. AD is a progressive, irreversible brain disorder that results in extensive neocortical and hippocampal neuronal loss and atrophy, amyloid beta (Aβ) protein-containing plaques and vascular deposition, tau-associated neurofibrillary tangles (NFT), neuroinflammation and severe cognitive impairment [6,7].

Distinguishing the earliest stages of AD from healthy ageing remains an area of great interest and a difficult diagnostic problem, although certain metrics, such as regional neuron loss and glial activation, have been established [1]. Age-related decline in neuron numbers is modest in the dentate gyrus and subiculum, while the CA1-CA3, entorhinal cortex, as well as the neocortex are preserved [8–12]. In striking contrast, AD brains exhibit profound neuronal death in the prefrontal and temporal cortex, entorhinal cortex, CA1 of the hippocampus, dentate gyrus and subiculum [8,9,13–17]. Another discriminating factor between ageing and AD is the severity of neuroinflammation, which is assessed, in part, by changes in glial density, activation and morphology [18]. Total glial density does not change in the human neocortex during the normal course of ageing or AD [19–21]. However, glial subtypes, such as microglia and astrocytes, are altered in both conditions [22,23]. As the brain's primary immune cell, microglia activate and proliferate with age in the neocortex, including the hippocampus and entorhinal cortex, of healthy humans [23,24]. AD brains display greater microglial activation and proliferation concomitant with Aβ plaques, particularly in the hippocampus [25–27]. Astrocytes provide metabolic and structural support to neurons, regulate neurogenesis, and modulate synaptic activity and neurotransmitter homeostasis [28]. Astrogliosis, as indicated by the upregulation of glial fibrillary acidic protein (GFAP), hypertrophy of the soma and cellular processes, and loss of domain organization, has been associated with normal ageing, and to a larger extent in AD [28–32].

Humans are considered uniquely susceptible to neurodegenerative disease, such as AD, but several recent studies have revealed AD-like pathology in the brains of non-human primates [33–37]. Aged lemurs, prosimians, monkeys and great apes exhibit diffuse and neuritic amyloid plaques as well as vascular amyloid, although cognitive changes based on plaque burden were not observed in aged macaques [34,35,38–46]. Furthermore, the presence of hyperphosphorylated tau has been reported in lemurs, squirrel and rhesus monkeys, baboons, and gorillas adjacent to Aβ deposition, and African green monkeys and aged chimpanzees exhibited NFT [34,35,46–49]. Closest in phylogeny to humans, non-human primates also exhibit senescence-related changes [33,50,51]. Mouse lemurs, marmosets, rhesus monkeys and apes show mild cognitive variations with age in spatial memory and executive function [52–57]. Some MRI studies in ageing mouse lemurs and rhesus macaques show progressive volumetric atrophy in the prefrontal cortex (PFC) and decreased brain weight in chimpanzees [55,58,59]. However, a more recent, comprehensive MRI analysis found no overt atrophy of volume in the neocortex and white matter in chimpanzees [51,59]. Postmortem analyses in primates have detected mild age-related dendritic atrophy, synapse loss, white matter damage, gliosis (i.e. activation of astrocytes and microglia), neurotransmitter alterations, and increases of Aβ in brain parenchyma and in cerebral vasculature [34,60–63].

Previous studies of ageing in non-human primates reported a lack of neuron loss in the neocortex, including CA1, entorhinal cortex and subiculum, with age [64–69]. Additionally, microglial activation has been observed in the frontal cortex, cingulum bundle and primary visual cortex, although numbers of activated microglia did not increase significantly with age in the visual cortex, substantia nigra and ventral tegmental area of aged rhesus monkeys [50,70,71]. Heightened expression of major histocompatibility complex class II (MHC-II) antigen, a marker of activated microglia, also was identified in the cerebral cortex and white matter of pig-tailed macaques [72]. Astrocyte activation in the form of higher GFAP expression was detected in the aged rhesus monkey hippocampus and PFC, although astrocyte density did not vary [73].

Formerly, we analysed the brains of 20 aged chimpanzees for evidence of Aβ and tau lesions as well as microglia and astrocyte activation [34,74,75]. Aβ was observed in plaques and, most predominantly, in blood vessels, which correlated with increased tau. Tau lesions were found in the form of AT8-immunoreactive (ir) pretangles, NFT and neuritic clusters (NC) of aggregated dystrophic neurites, and NFT were observed in apes that exhibited plaques and moderate or severe cerebral amyloid angiopathy (CAA), a condition in which amyloid accumulates in the brain's vasculature. Age correlated with greater volumes of Aβ plaques and vessels, but not tau or activated microglia and astrocyte densities. Like AD, Aβ42 deposition was positively associated with higher hippocampal microglial activation in chimpanzees, while astrogliosis occurred in both the hippocampus and PFC layer I in conjunction with Aβ and tau proteins. Contrary to AD, activated microglia density was not significantly correlated with tau lesions and astrogliosis was not identified in other cortical layers in chimpanzees. Despite certain comparable age-related and AD-like pathologies identified in non-human primate brains, only humans exhibit major neuronal loss and severe cognitive decline as observed in clinical AD. Thus, building on our prior investigations, we quantified regional neuron density, glia density, and glia:neuron ratios in the dorsolateral PFC, middle temporal gyrus (MTG), and CA1 and CA3 hippocampal subfields of chimpanzees to determine if ageing or AD pathology correlates with regional neuron loss or glial activation.

2. Material and methods

(a) Specimens and sample processing

Postmortem brain samples from 12 male (ages 17–62 years) and 16 female (ages 12–58 years) chimpanzees (*Pan troglodytes*, electronic supplementary material, table S1) were acquired from Association of Zoos and Aquariums-accredited zoos and American Association for Accreditation of Laboratory Animal Care-accredited research institutions through the National Chimpanzee Brain Resource (NIH grant: NS092988). The chimpanzees included in this study did not participate in formal behavioural or cognitive testing and were maintained in accordance with each institution's animal care and use guidelines. Available health information for each animal has been included in electronic supplementary material, table S2. Depending on availability, samples were taken from the right or left hemispheres. Brains were collected postmortem after death from natural causes (approximately less than or equal to 20 h PMI), immersion-fixed in 10% buffered formalin for a minimum of 10 days, and transferred to a 0.1 M buffered

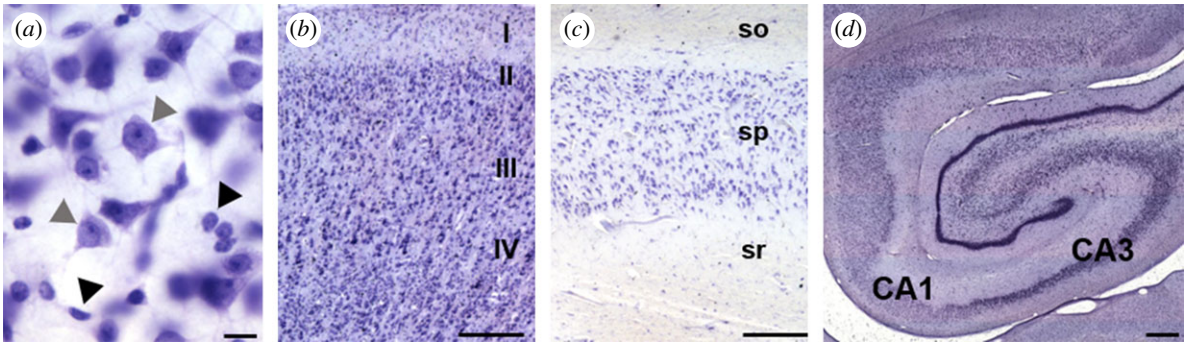

Figure 1. Photomicrographs of Nissl staining in the chimpanzee brain: (*a*) classification of neurons (grey arrowhead) and glia (black arrowhead), (*b*) layer III in the MTG, (*c*) stratum pyramidale layer of the CA1 and (*d*) a photo montage delineating the CA1 and CA3 hippocampal subfields. Abbreviations: so, stratum oriens; sp, stratum pyramidale; sr, stratum radiatum. Scale bar = 25 µm (*a*), 250 µm (*b–d*). (Online version in colour.)

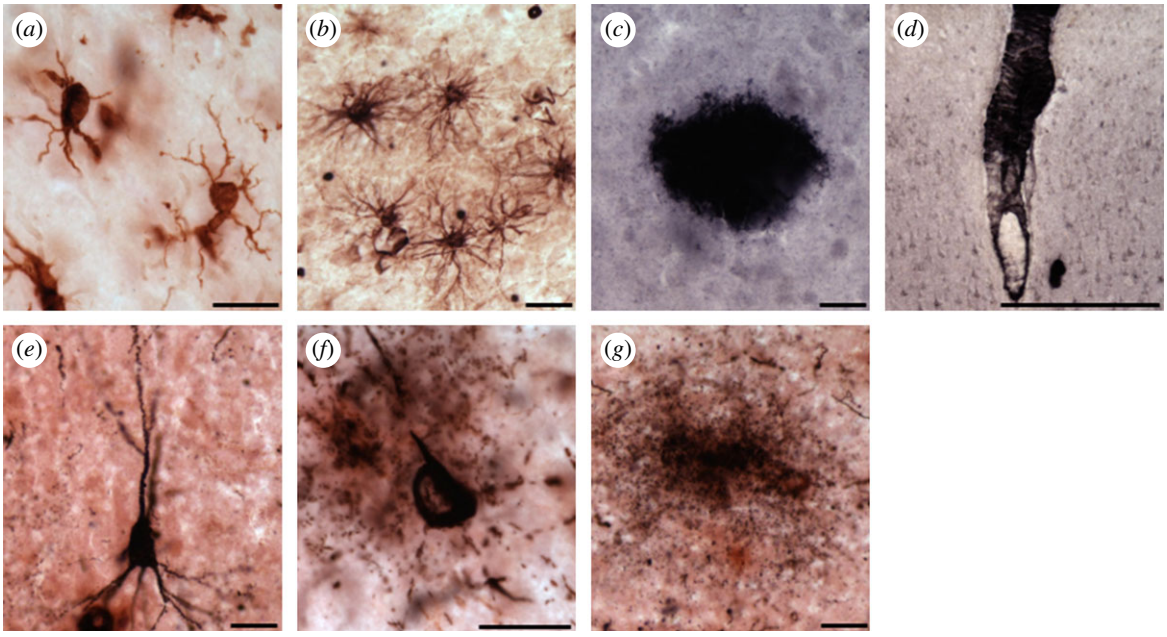

Figure 2. Photomicrographs of Iba1-ir microglia (*a*), GFAP-ir astrocytes (*b*), Aβ42-ir plaque (*c*), leptomeningeal vessel (*d*), AT8-ir pretangle (*e*), NFT (*f*) and tau neuritic cluster (*g*) in the chimpanzee PFC (*a–d,f*) and hippocampus (*e,g*). Scale bars = 25 µm (*a–c,e–g*), 250 µm (*d*). (Online version in colour.)

saline solution containing 0.1% sodium azide at 4°C for storage. Samples were cryoprotected in a graded series of sucrose solutions (10, 20 and 30%) and cut frozen into 40 µm-thick sections in a coronal plane using a Leica SM2000R freezing sliding microtome (Buffalo Grove, IL). Sections then were placed into individual centrifuge tubes containing a cryo-protection solution (30% dH_2O, 30% ethylene glycol, 30% glycerol, 10% 0.244 M phosphate-buffered saline (PBS)), numbered sequentially, and stored at −20°C until histological or immunohistochemical processing. Every 10th section in each region was stained for Nissl substance with a 0.5% cresyl violet solution to reveal cell somata, define cytoarchitectural boundaries, and quantify neuron density (Nv), glia density (Gv) and glia to neuron (G : N) ratio (figure 1). Previously, immunohistochemistry was performed for markers of hyperphosphorylated tau (AT8), Aβ42, microglia (Iba1, ionized calcium-binding adaptor molecule 1), and astrocytes (GFAP, glial fibrillary acidic protein) in the same regions using the avidin-biotin-peroxidase method and 3,3′-diaminobenzidine (DAB) with nickel enhancement or NovaRed (figure 2) [34].

(b) Regions of interest

We analysed layer III in Brodmann's areas 9 and 10 of the dorsolateral PFC and Brodmann's area 21 of the MTG, as well as the stratum pyramidale in the hippocampal subfields CA1 and CA3 (figure 1). Sampled areas were selected based on prior reports that demonstrated involvement of these regions in both ageing and AD pathology [76–78]. Humans with AD display extensive neuron and synapse loss in layers III and V of the neocortex and stratum pyramidale in the CA1 field, and neuritic Aβ plaques and NFT are most prevalent in these cortical layers [5,16,17,79,80]. Chimpanzees also display Aβ and tau pathologies in the neocortex and hippocampus [34,40].

(c) Stereologic data acquisition

Quantitative analyses were performed using computer-assisted stereology with an Olympus BX-51 photomicroscope equipped with a digital camera and StereoInvestigator software v. 11 (MBF Bioscience, Williston, VT) by two observers blinded to age, sex and pathology. Initial subsampling techniques were performed for each probe to determine appropriate sampling parameters [81]. Regional Nv and Gv were obtained using the optical fractionator probe at 40× (N.A. 0.75) under Köhler illumination. Counting frames were set at 100 × 100 µm with a grid size of 250 × 250 µm, a disector height of 7 µm, and a guard zone of 2%. Beginning at a random starting point, three equidistant sections (every 10th section) per region of interest and animal were selected for analysis. A marker was placed on the nucleus of neurons and on glia when encountered within the optical

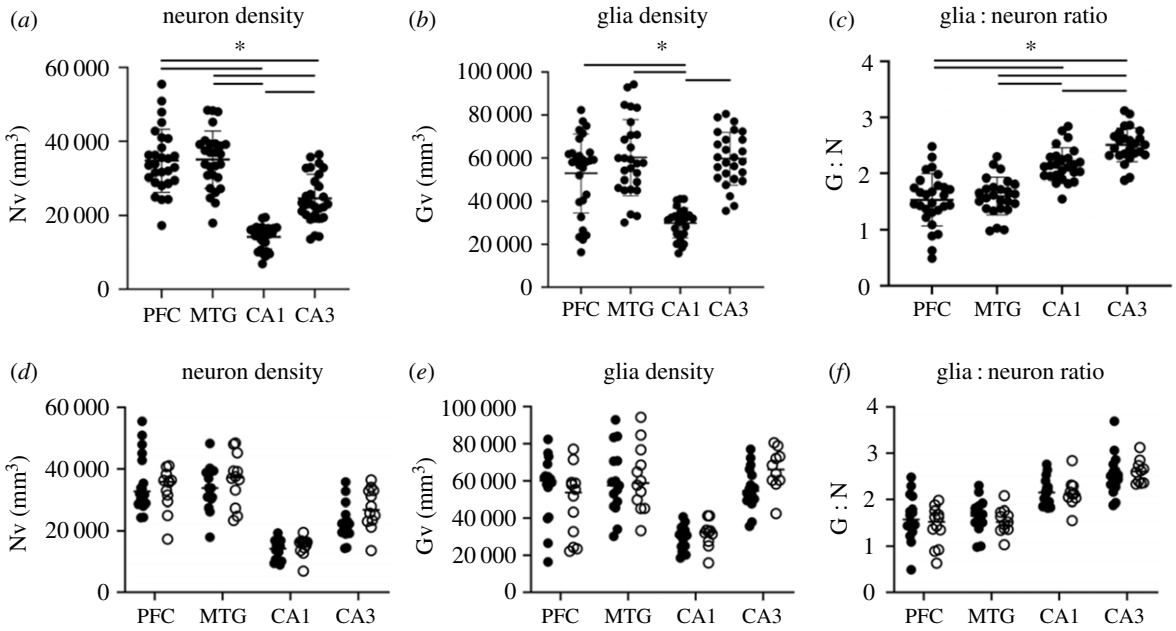

Figure 3. Scatter plots of regional neuron density (*a*), glia density (*b*) and glia:neuron ratios (*c*) in the chimpanzee brain. Although variations were found by region (*a–c*), sex differences were not observed (*d–f*; solid circle, females; open circle, males). *$p \leq 0.05$.

disector frame, and mounted section thickness was measured at every fifth sampling site. Neurons were identified by the presence of a nucleus, nucleolus and axonal hillock, while glia were distinguished by their lack of nuclei and granules of heterochromatin, giving a speckled appearance. For each region, Nv and Gv (per mm^3) were calculated as the population estimate divided by sum volume of the examined disectors, and the G : N ratio was calculated as Gv/Nv [82]. The percentage (%) of gain or loss between old and young animals was determined with the following equation: (aged density or ratio/young density or ratio × 100) − 100. To correct for tissue shrinkage in the *z*-axis, the height of the disector was multiplied by the ratio of section thickness to the actual weighted mean thickness after mounting and dehydration. No correction was necessary for the *x* and *y* dimensions, because shrinkage in section surface area is minimal [83]. The mean number of sampling sites per individual was 32 ± 6 (mean ± s.d.) for PFC and MTG and 65 ± 7 for the CA1 and CA3. The mean number of markers per individual for neurons was 375 ± 97 and for glia was 610 ± 227 in the PFC and MTG. In the CA1 and CA3, the mean number of markers per individual for neurons was 397 ± 33 and for glia was 960 ± 72. The average CE for all regional neuron densities was 0.06 and for glia densities was 0.05.

(d) Statistical analyses

Data were previously collected for Aβ42 plaque and vessel volume (%), AT8-immunoreactive (ir) pretangle, NFT and tau NC densities, Iba1-ir microglia densities, and GFAP-ir astrocyte densities from aged apes (i.e. greater than or equal to 37 years old; figure 2) [34,74,75]. Young chimpanzees (i.e. greater than or equal to 35 years) were assessed for AD pathology, which was absent with the exception of a few AT8-ir pretangles in the PFC of one 12-year-old female that died from peritonitis, and Iba1-ir microglia densities and GFAP-ir astrocyte densities [34,74,75]. All pathology densities and volumes were checked for linearity, and because of skewness of means close to zero, densities and volumes were transformed using the formula: arcsin (sqrt (density/1000)). To evaluate neuropathologic changes for each individual, a brain age value from 0 to 60 was computed using a pathology scoring system adapted from staging guidelines for Aβ and NFT deposition in AD and CAA [34]. Principal component analysis (PCA) was performed to reduce the number of pathological variables to the most relevant factors for brain age in chimpanzees. Four factors—AT8-ir NC densities, NFT density, and AB plaque and vessel volumes—explained 57% of the variance, and all variables had primary loadings between 0.67 and 0.87. Regression factors (PCA-generated pathology factor) created from this prior analysis were employed for further regression analyses with Nv and Gv in this study. Data were tested for a normal distribution and for outliers using the ROUT method ($Q = 1$), and outliers were excluded. Linear regression analyses were used to determine relationships between the dependent variables of regional Nv, Gv and G : N, and independent variables of chronological age, PCA-generated pathology factor, Aβ42 plaque and vessel volumes (%), and pretangle, NFT, and tau NC densities (per mm^3). Sex and brain region variations were examined using two-way (sex) or mixed model (region) ANOVAs with Bonferroni post hoc tests. Statistical analyses were conducted using GraphPad Prism 8.3.0 (San Diego, CA), and the level of significance (α) was set at 0.05.

3. Results

Regional Nv, Gv and G : N were quantified for layer III of the PFC and MTG as well as the pyramidal layer of the CA1 and CA3 hippocampal subfields (figure 1). Average densities and ratios for young ($n = 8$, 12–35 years), aged ($n = 20$, 37–62 years), and all chimpanzees in addition to the per cent gain or loss between old and young animals for each region and variable are shown in electronic supplementary material, table S3. Using previously collected microglia and astrocyte densities from tissue in the same animals, along with the total glia density from the current study, the breakdown of glial subtypes was calculated for each region examined with an average across all areas of 81% oligodendrocytes, 8% astrocytes and 11% microglia (electronic supplementary material, table S4) [74,75].

(a) Region and sex

Mixed model ANOVA with Bonferroni multiple comparison tests revealed that PFC and MTG Nv are significantly higher than CA1 (PFC: $t_{27} = 12.01$, MTG: $t_{26} = 13.54$, $ps \leq 0.01$) and CA3 (PFC: $t_{27} = 4.97$, MTG: $t_{26} = 5.97$, $ps \leq 0.01$) but do not differ from each other ($t_{26} = 0.17$, $p = 0.99$; figure 3*a*). CA3 Nv

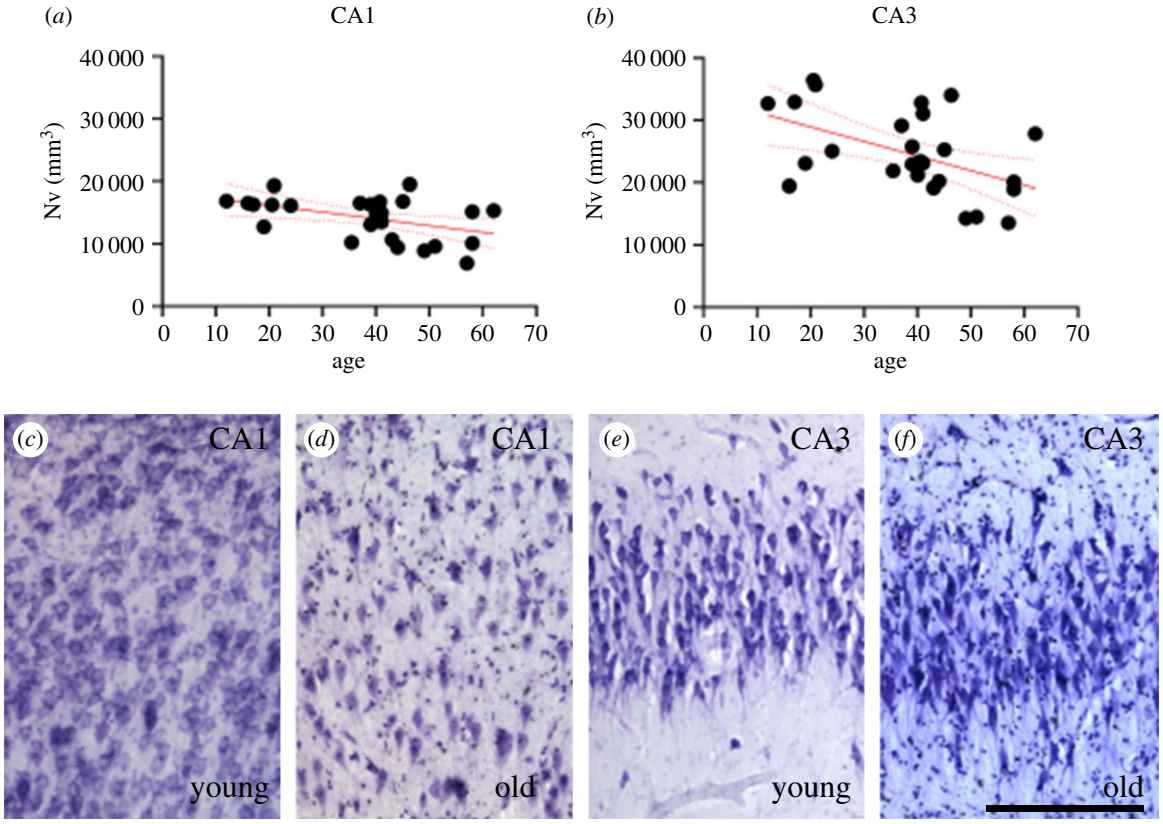

Figure 4. A decrease in CA1 and CA3 neuron densities (Nv, mm^3; *a*,*b*) was correlated with older age in the chimpanzee brain ($ps \leq 0.02$). Photomicrographs of Nissl staining in hippocampal subfields CA1 (*c*,*d*) and CA3 (*e*,*f*) in a young chimpanzee (*c*,*e*) and an old (*d*,*f*) chimpanzee brain. Scale bar = 250 µm. (Online version in colour.)

was higher than CA1 ($t_{27} = 12.44$, $p \leq 0.01$). Glia density was significantly higher in the PFC and MTG than CA1 (PFC: $t_{25} = 5.77$, MTG: $t_{24} = 8.69$, $ps \leq 0.01$), but not CA3 (PFC: $t_{25} = 1.43$, MTG: $t_{24} = 0.11$, $ps \geq 0.99$; figure 3*b*). PFC Gv did not vary from MTG ($t_{26} = 2.14$, $p = 0.25$). As with Nv, CA3 Gv was greater than CA1 ($t_{25} = 16.26$, $p \leq 0.01$). Both PFC and MTG G : N ratios were significantly lower than CA1 (PFC: $t_{25} = 5.14$, MTG: $t_{22} = 5.94$, $ps \leq 0.01$) and CA3 (PFC_{24}: $t = 8.18$, MTG: $t_{21} = 9.48$, $ps \leq 0.01$), while CA3 was significantly greater than CA1 ($t_{24} = 5.76$, $p \leq 0.01$; figure 3*c*). G : N in the PFC did not differ from MTG ($t_{24} = 1.01$, $p = 0.99$). Two-way ANOVA revealed no sex differences in Nv ($F_{1,103} = 1.61$, $p = 0.21$), Gv ($F_{1,99} = 0.24$, $p = 0.63$) or G : N ($F_{1,97} = 0.61$, $p = 0.44$; figure 3*d–f*) for any region examined.

(b) Age

Age was associated with significantly decreased Nv in both CA1 and CA3 (figure 4, $ps \leq 0.02$; electronic supplementary material, table S5). Age-related changes were not observed in PFC or MTG Nv (electronic supplementary material, figure S1A-B, $ps \geq 0.29$). There were no age-related changes for Gv (electronic supplementary material, figure S1C-F, $ps \geq 0.07$), or G : N in any of the regions examined (electronic supplementary material, figure S1G-J, $ps \geq 0.10$; electronic supplementary material, table S5).

(c) Alzheimer's disease pathology

To determine an overall Aβ and tau score for each chimpanzee, a PCA-generated pathology factor was calculated as previously described [34]. Linear regression analyses were used to investigate the association of regional Nv, Gv or GN with PCA-generated pathology factors and regional AD pathology measurements previously collected in the 20 oldest apes (i.e. greater than or equal to 37 years [34]). Pathologic markers included Aβ42-ir plaque and vessel volumes (%) and AT8-ir pretangle, NFT and NC densities (per mm^3) collected in the PFC, MTG, CA1 and CA3. Briefly, plaques were defined as extracellular accumulations of insoluble Aβ42, while vascular amyloid was quantified when Aβ42 deposition was present in the vessel walls. Pretangles were characterized as having an intact cell soma, the presence of diffuse punctate hyperphosphorylated tau (AT8) immunostaining in the cytoplasm, well-preserved dendrites and a nucleus. NFT were identified based on intraneuronal aggregates of hyperphosphorylated tau, and distorted, shortened or absent dendrites and axons. Tau NC contained clusters of dystrophic neurites, consisting of AT8-ir swollen axons and dendrites, or diffuse, punctate staining.

Regional Nv, Gv and G : N were not correlated with PCA-based pathology factors or AD pathologies with two exceptions (electronic supplementary material, table S6, $ps \geq 0.07$). In the MTG only, Aβ42 vessel volume was associated with decreased Nv ($R^2 = 0.23$, $p = 0.05$; electronic supplementary material, figure S2A), even after excluding two outliers with significantly high levels of amyloid deposition ($R^2 = 0.28$, $p = 0.04$; electronic supplementary material, figure S2B,E-F). However, to correct for multiple comparison testing error, we performed a Bonferroni correction ($p = 0.002$), and the correlation of MTG Aβ42 vessel volume and Nv was no longer significant. Additionally, pretangle density was negatively correlated with Nv in the CA1 ($R^2 = 0.19$, $p = 0.05$; electronic supplementary material, figure S2C), but after removal of two outliers with high pretangle numbers, the association was non-significant ($R^2 = 0.00$, $p = 0.88$; electronic supplementary material, figure S2D,G-H).

4. Discussion

Several studies identified senescence-related changes and AD-like pathology in the brains of non-human primates [33–35,37,38]. Yet, none established whether Aβ or tau pathologies were associated with the profound neuron loss and neuroinflammation observed in the human AD brain. To address this knowledge gap, we quantified Nv, Gv and G : N in postmortem tissue obtained from a large cohort of chimpanzee brains with markers of AD pathology.

Neuron density decreased moderately with age in the CA1 (12%) and CA3 (19%) hippocampal subfields in this sample of chimpanzees. These data diverge from prior investigations in older non-human primates and humans [5,12,65,84]. Previously, no changes in neuron number with age were found in CA1 and CA3 for chimpanzees and rhesus macaques [65,84]. However, both studies were limited in the number of animals (chimpanzees = 6; macaques = 8) compared to the current study of 28 apes. Neuron numbers were reported rather than densities, and both the polymorphic and pyramidal layers were measured in macaques. In elderly humans, the majority of studies of CA1 and CA3 neurons demonstrated preservation during physiological ageing [5,9,10,12,85]. Although the human and chimpanzee hippocampus appears to be differentially affected by ageing, this region is vulnerable to neuronal death in both species with age and neurodegeneration.

A non-significant trend of neuron loss (20-24%) was associated with Aβ42 vascular deposition in the temporal cortex of chimpanzees. Previously, we found that Aβ42 was threefold higher in neocortical vessels compared to the hippocampus [34]. In addition, Aβ plaque and vessel volumes were significantly greater in older apes, suggesting that age-related increases contribute to neuronal toxicity in MTG of aged chimpanzees. This concept is further supported by the lack of neuron loss with age in this region. Notably, pretangle densities were highest in the MTG compared to the hippocampus, although pretangles did not correlate with neuron loss [34,40]. AD pathologic markers in great apes demonstrate similar regional staging progression as humans with Aβ deposits occurring first in the neocortex, whereas NFT initiate in the medial temporal lobe and brainstem [86,87]. Thus, MTG may represent an area in which Aβ and tau pathologies converge in chimpanzees. Moreover, MTG exhibits the largest, albeit nonsignificant, decrease in Gv (18%) and G : N (34%) with age and the lowest density of microglia in these apes (electronic supplementary material, table S3). In AD, microglia play an important role in the removal of Aβ peptides through phagocytosis, and physiological senescence in microglia is accompanied by the release of inflammatory cytokines, which have detrimental effects on neurons [88]. Consequently, in chimpanzees, the low number of microglia in MTG may result in decreased Aβ42 phagocytosis, exacerbated by an age-associated increase in Aβ42-ir vasculature and high numbers of pretangles, leading to neuronal death.

Humans with AD differ from chimpanzees in that significant neuronal loss occurs in the PFC and CA1 as well as the temporal cortex [5,14,16,89,90]. The absence of cell death in the chimpanzee hippocampus could be due to the increase in severity of NFT pathology in AD relative to milder NFT densities in aged chimpanzees. In AD, NFT correlates strongly with neuronal loss and cognitive decline [91,92]. Therefore, we compared CA1 Nv in apes with pretangles (13 581 mm^{-3}) or NFT (115 959 mm^{-3}) to those without (15 025 mm^{-3}), and observed a trend of mild decline with tau pathologies. Moreover, a 57-year-old male chimpanzee with the highest CA1 pretangle and NFT densities exhibited the lowest Nv (6902 mm^{-3}) of all the apes and was an outlier in our original analysis, which showed a negative correlation of CA1 pretangle density and Nv (electronic supplementary material, figure S2C). Once this animal was removed, the association no longer remained (electronic supplementary material, figure S2D). Furthermore, like humans, Aβ plaque and vascular levels were higher in the neocortical regions compared to the hippocampal subfields in these chimpanzees.

Neocortical and hippocampal glia densities were not associated with age or AD pathology in chimpanzees. Our previous findings support the lack of age and pathology-related variation in microglia and astrocyte densities in the same apes and brain regions [74,75]. Human studies also found that astrocyte numbers did not change with age or AD pathology, and microglia density did not differ in the temporal cortex of control and AD brains [19,20,93]. Instead, expression of GFAP and MHC-II, markers of astrocyte and microglia activation, increased in AD patients, implicating a phenotypic change instead of a marked proliferation [93]. Greater microglial activation was also detected in the hippocampus in elderly non-demented subjects [23]. Non-human primates demonstrate a similar pattern. Rhesus monkeys exhibited both senescence-associated expression of MHC-II and activated microglia concomitant with fibrillar Aβ plaques with clusters of phosphorylated tau-containing swollen neurites [72,94,95]. Likewise, Aβ oligomers trigger astrocyte and microglial activation in long-tailed macaques, and microglial activation was observed in the brains of aged common marmosets in conjunction with Aβ and hyperphosphorylated tau deposition [46,96]. In chimpanzees, greater volumes of Aβ42 plaque and vessel deposition were correlated with higher hippocampal microglial activation, while tau deposition was significantly increased in activated, intermediate microglia [34]. This evidence suggests that overall glia densities are not impacted by age or AD pathology in great apes, although glial activation increases in proximity to Aβ and tau deposition.

Unexpectedly, the breakdown of glial subtypes in chimpanzees (81% oligodendrocytes, 8% astrocytes and 11% microglia) diverges from estimates in humans (males: 75% oligodendrocytes, 20% astrocytes, 5% microglia), who have a higher percentage of astrocytes and lower percentage of microglia [20]. Rhesus monkey brains have a distribution of 35% oligodendrocytes, 57% astrocytes and 7% microglial cells in the cortex [97]. Although potentially a result of different quantification methods, the species-related variation in glial makeup may be an important difference in humans and could play a role in the reduced neuroinflammation observed in ape brains during ageing, although further analyses are required.

Glia : neuron ratios were not associated with age or pathology in chimpanzees. Average G : N were higher in the hippocampus (2.36) compared to the neocortex (1.57). These results are in accordance with previous studies in other non-human primates and humans. A neocortical G : N of 1.70 was reported in rhesus monkeys and 1.98 in chimpanzees, while human cortical grey matter ranges from 0.6 to 4.0 with an average of 1.79 [72,98,99]. In addition, a G : N of 1.37 was found in the neocortex of AD patients and controls, suggesting the ratio does not change with disease [21].

Table 1. Summary of neuropathologic changes in ageing and Alzheimer's disease in chimpanzees and humans.

	Alzheimer's disease		ageing	
pathology	**chimpanzee**	**human**	**chimpanzee**	**human**
Aβ	Aβ is primarily in blood vessels and occurs prior to plaque formation	Aβ is primarily in plaques, although CAA occurs in 80% of AD patients	chimpanzees demonstrate increased intravascular Aβ deposition with age	humans exhibit increased Aβ deposition in plaques and vessels with age
	Aβ pathology is associated with increased tau pathology			
tau	neuritic clusters contain dystrophic tau neurites but lack an Aβ core	neuritic plaques contain an Aβ core	pretangles in the neocortex increase with age	NFT increase with age in the hippocampus
neuro-inflammation	Aβ42 is correlated with increased microglial activation (i.e. plaques in humans, vessels in chimpanzees)		age is not associated with increased microglial or astrocyte density or activation in chimpanzees	humans display both increased microglial activation and density with age
	microglial activation is correlated with Aβ but not NFT lesions	microglial activation is associated with Aβ and NFT pathology		
neuron loss	neuron loss occurs in the temporal cortex in association with Aβ deposition in the brain's blood vessels	selective neuronal loss occurs in the prefrontal cortex and hippocampus	neuron loss was observed in the hippocampus of chimpanzees	selective neuronal loss occurs in the subiculum and dentate gyrus but not CA1-CA3 subfields
cognitive impairment	antemortem cognitive testing in chimpanzees with AD pathology has not been performed yet	severe memory, cognitive and behavioural deficits are observed	cognitive testing is rare in aged apes; mild cognitive deficits in spatial memory, attention, executive function, and cognitive flexibility have been noted	processing speed, attention, memory and cognitive flexibility gradually decline during ageing

Comparing differences in the brains of humans and great apes can enhance our understanding of the selective vulnerability of humans to neurodegenerative diseases, such as AD (table 1). In the current study, we found that chimpanzees experience limited decreases in Nv in association with physiologic and pathologic ageing, although not to the same severity as AD. A caveat of this investigation, though, is the lack of antemortem cognitive testing, which is necessary to determine whether neuronal loss is associated with cognitive decline in aged chimpanzees. Moreover, the contribution of life-history factors, such as social environment, diet, body metabolism and physical activity, that may affect neurological variation were not examined in these animals. These data highlight and further support the role for non-human primates as models of ageing and neurodegenerative diseases due to their long lifespans, genomic similarities, and complex physiology and cognition.

Ethics. All samples were acquired postmortem from American Zoo and Aquarium-accredited zoos and American Association for Accreditation of Laboratory Animal Care-accredited research institutions through the National Chimpanzee Brain Resource.

Data accessibility. Data will be available on the National Chimpanzee Brain Resource website: https://www.chimpanzeebrain.org.

Authors' contributions. All authors have approved this manuscript. M.K.E., P.R.H. and M.A.R. designed research; C.C.S., W.D.H., J.J.E., J.M.E. and P.R.H. provided samples; M.K.E. and E.L.M. collected data; M.K.E., R.S.M. and M.A.R. analysed data; and M.K.E., C.C.S., R.S.M., W.D.H., J.J.E., J.M.E., E.J.M., P.R.H. and M.A.R. wrote the manuscript.

Competing interests. The authors declare no competing interests.

Funding. This work was supported and funded by the NSF (BCS-1316829, M.A.R.), NIH (NS042867, NS073134, NS092988, W.D.H., C.C.S.; AG017802, J.J.E.; AG014308, J.M.E.; AG005138, P.R.H.; AG014449, AG043375, E.J.M.), James S. McDonnell Foundation (220020293, C.C.S.), Sigma Xi (M.K.E.), KSU Research Council (M.A.R.) and KSU Graduate Student Senate (M.K.E.).

Acknowledgements. We thank Cheryl Stimpson and Bridget Wicinski for their technical assistance.

References

1. Toepper M. 2017 Dissociating normal aging from Alzheimer's disease: a view from cognitive neuroscience. *J. Alzheimers Dis.* **57**, 331–352. (doi:10.3233/JAD-161099)
2. Hedman AM, van Haren NEM, Schnack HG, Kahn RS, Hulshoff Pol HE. 2012 Human brain changes across the life span: a review of 56 longitudinal magnetic resonance imaging studies. *Hum. Brain Mapp.* **33**, 1987–2002. (doi:10.1002/hbm.21334)
3. Morgan DG. 1987 The dopamine and serotonin systems during aging in human and rodent brain. A brief review. *Prog. Neuro-Psychopharmacol. Biol. Psychiat.* **11**, 153–157. (doi:10.1016/0278-5846(87)90053-4)
4. Masliah E, Mallory M, Hansen L, DeTeresa R, Terry RD. 1993 Quantitative synaptic alterations in the human neocortex during normal aging. *Neurology* **43**, 192–197. (doi:10.1212/WNL.43.1_Part_1.192)
5. West MJ, Coleman PD, Flood DG, Troncoso JC. 1994 Differences in the pattern of hippocampal neuronal loss in normal ageing and Alzheimer's disease. *Lancet* **344**, 769–772. (doi:10.1016/S0140-6736(94)92338-8)
6. Serrano-Pozo A, Frosch MP, Masliah E, Hyman BT. 2011 Neuropathological alterations in Alzheimer disease. *Cold Spring Harb. Perspect. Med.* **1**, a006189. (doi:10.1101/cshperspect.a006189)
7. Heppner FL, Ransohoff RM, Becher B. 2015 Immune attack: the role of inflammation in Alzheimer disease. *Nat. Rev. Neurosci.* **16**, 358–372. (doi:10.1038/nrn3880)
8. Gómez-Isla T, Price JL, McKeel Jr DW, Morris JC, Growdon JH, Hyman BT. 1996 Profound loss of layer II entorhinal cortex neurons occurs in very mild Alzheimer's disease. *J. Neurosci.* **16**, 4491–4500. (doi:10.1523/JNEUROSCI.16-14-04491.1996)
9. Simić G, Kostović I, Winblad B, Bogdanović N. 1997 Volume and number of neurons of the human hippocampal formation in normal aging and Alzheimer's disease. *J. Comp. Neurol.* **379**, 482–494. (doi:10.1002/(SICI)1096-9861(19970324)379:4<482::AID-CNE2>3.0.CO;2-Z)
10. Terry RD, Deteresa R, Hansen LA. 1987 Neocortical cell counts in normal human adult aging. *Ann. Neurol.* **21**, 530–539. (doi:10.1002/ana.410210603)
11. Pakkenberg B, Gundersen HJG. 1997 Neocortical neuron number in humans: effect of sex and age. *J. Comp. Neurol.* **384**, 312–320. (doi:10.1002/(SICI)1096-9861(19970728)384:2<312::AID-CNE10>3.0.CO;2-K)
12. Martínez-Pinilla E, Ordóñez C, del Valle E, Navarro A, Tolivia J. 2016 Regional and gender study of neuronal density in brain during aging and in Alzheimer's disease. *Front. Aging Neurosci.* **8**, 1–12. (doi:10.3389/fnagi.2016.00213)
13. Morrison JH, Hof PR. 1997 Life and death of neurons in the aging brain. *Science* **278**, 412–419. (doi:10.1126/science.278.5337.412)
14. Gomez-Isla T, Hollister R, West H, Mui S, Growdon JH, Petersen RC, Parisi JE, Hyman BT. 1997 Neuronal loss correlates with but exceeds neurofibrillary tangles in Alzheimer's disease. *Ann. Neurol.* **41**, 17–24. (doi:10.1002/ana.410410106)
15. West MJ, Kawas CH, Stewart WF, Rudow GL, Troncoso JC. 2004 Hippocampal neurons in pre-clinical Alzheimer's disease. *Neurobiol. Aging* **25**, 1205–1212. (doi:10.1016/j.neurobiolaging.2003.12.005)
16. Giannakopoulos P, Hof PR, Kovari E, Vallet PG, Herrmann FR, Bouras C. 1996 Distinct patterns of neuronal loss and Alzheimer's disease lesion distribution in elderly individuals older than 90 years. *J. Neuropathol. Exp. Neurol.* **55**, 1210–1220. (doi:10.1097/00005072-199612000-00004)
17. Bussière T, Gold G, Kövari E, Giannakopoulos P, Bouras C, Perl DP, Morrison JH, Hof PR. 2003 Stereologic analysis of neurofibrillary tangle formation in prefrontal cortex area 9 in aging and Alzheimer's disease. *Neuroscience* **117**, 577–592. (doi:10.1016/S0306-4522(02)00942-9)
18. Meraz Rios MA, Toral-Rios D, Franco-Bocanegra D, Villeda-Hernández J, Campos-Peña V. 2013 Inflammatory process in Alzheimer's disease. *Front. Integr. Neurosci.* **7**, 59. (doi:10.3389/fnint.2013.00059)
19. Pakkenberg B, Pelvig D, Marner L, Bundgaard MJ, Gundersen HJG, Nyengaard JR, Regeur L. 2003 Aging and the human neocortex. *Exp. Gerontol.* **38**, 95–99. (doi:10.1016/S0531-5565(02)00151-1)
20. Pelvig DP, Pakkenberg H, Stark AK, Pakkenberg B. 2008 Neocortical glial cell numbers in human brains. *Neurobiol. Aging* **29**, 1754–1762. (doi:10.1016/j.neurobiolaging.2007.04.013)
21. Pelvig DP, Pakkenberg H, Regeur L, Oster S, Pakkenberg B. 2003 Neocortical glial cell numbers in Alzheimer's disease. A stereological study. *Dement. Geriatr. Cogn. Disord.* **16**, 212–219. (doi:10.1159/000072805)
22. Von Bernhardi R, Tichauer JE, Eugenin J. 2010 Aging-dependent changes of microglial cells and their relevance for neurodegenerative disorders. *J. Neurochem.* **112**, 1099–1114. (doi:10.1111/j.1471-4159.2009.06537.x)
23. DiPatre PL, Gelman BB. 1997 Microglial cell activation in aging and Alzheimer disease: partial linkage with neurofibrillary tangle burden in the hippocampus. *J. Neuropathol. Exp. Neurol.* **56**, 143–149. (doi:10.1097/00005072-199702000-00004)
24. Schuitemaker A *et al.* 2012 Microglial activation in healthy aging. *Neurobiol. Aging* **33**, 1067–1072. (doi:10.1016/j.neurobiolaging.2010.09.016)
25. Ekonomou A *et al.* 2015 Stage-specific changes in neurogenic and glial markers in Alzheimer's disease. *Biol. Psychiatry* **77**, 711–719. (doi:10.1016/j.biopsych.2014.05.021)
26. Meda L, Cassatella MA, Szendrei GI, Otvos LJ, Baron P, Villalba M, Ferrari D, Rossi F. 1995 Activation of microglial cells by beta-amyloid protein and

interferon-gamma. *Nature* **374**, 647–650. (doi:10.1038/374647a0)

27. Rozemuller AJM, van Gool WA, Eikelenboom P. 2005 The neuroinflammatory response in plaques and amyloid angiopathy in Alzheimer's disease: therapeutic implications. *Curr. Drug Targets CNS Neurol. Disord.* **4**, 223–233. (doi:10.2174/1568007054038229)
28. Dossi E, Vasile F, Rouach N. 2018 Human astrocytes in the diseased brain. *Brain Res. Bull.* **136**, 139–156. (doi:10.1016/j.brainresbull.2017.02.001)
29. Rozovsky I, Finch CE, Morgan TE. 1998 Age-related activation of microglia and astrocytes: *in vitro* studies show persistent phenotypes of aging, increased proliferation, and resistance to down-regulation. *Neurobiol. Aging* **19**, 97–103. (doi:10.1016/S0197-4580(97)00169-3)
30. Sofroniew MV, Vinters HV. 2010 Astrocytes: biology and pathology. *Acta Neuropathol.* **119**, 7–35. (doi:10.1007/s00401-009-0619-8)
31. Beach TG, Walker R, McGeer EG. 1989 Patterns of gliosis in Alzheimer's disease and aging cerebrum. *Glia* **2**, 420–436. (doi:10.1002/glia.440020605)
32. Cotrina ML, Nedergaard M. 2002 Astrocytes in the aging brain. *J. Neurosci. Res.* **67**, 1–10. (doi:10.1002/jnr.10121)
33. Hof PR, Gilissen EP, Sherwood CC. 2002 Comparative neuropathology of brain aging in primates. In *Aging in nonhuman primates* (eds JM Erwin, PR Hof), pp. 130–154. Basel, Switzerland: Karger.
34. Edler MK, Sherwood CC, Meindl RS, Hopkins WD, Ely JJ, Erwin JM, Mufson EJ, Hof PR, Raghanti MA. 2017 Aged chimpanzees exhibit pathologic hallmarks of Alzheimer's disease. *Neurobiol. Aging* **59**, 107–120. (doi:10.1016/j.neurobiolaging.2017.07.006)
35. Cramer PE *et al.* 2018 Aging African green monkeys manifest transcriptional, pathological, and cognitive hallmarks of human Alzheimer's disease. *Neurobiol. Aging* **64**, 92–106. (doi:10.1016/j.neurobiolaging.2017.12.011)
36. Mufson EJ, Benzing WC, Cole GM, Wang H, Emerich DF, Sladek JR, Morrison JH, Kordower JH. 1994 Apolipoprotein E-immunoreactivity in aged rhesus monkey cortex: colocalization with amyloid plaques. *Neurobiol. Aging* **15**, 621–627. (doi:10.1016/0197-4580(94)00064-6)
37. Perez SE, Sherwood CC, Cranfield MR, Erwin JM, Mudakikwa A, Hof PR, Mufson EJ. 2016 Early Alzheimer's disease-type pathology in the frontal cortex of wild mountain gorillas (*Gorilla beringei beringei*). *Neurobiol. Aging.* **39**, 195–201. (doi:10.1016/j.neurobiolaging.2015.12.017)
38. Gearing M, Tigges J, Mori H, Mirra SS. 1996 Aβ40 is a major form of β-amyloid in nonhuman primates. *Neurobiol. Aging* **17**, 903–908. (doi:10.1016/S0197-4580(96)00164-9)
39. Gearing M, Rebeck GW, Hyman BT, Tigges J, Mirra SS. 1994 Neuropathology and apolipoprotein E profile of aged chimpanzees: implications for Alzheimer disease. *Proc. Natl Acad. Sci. USA* **91**, 9382–9386. (doi:10.1073/pnas.91.20.9382)
40. Rosen RF *et al.* 2008 Tauopathy with paired helical filaments in an aged chimpanzee. *J. Comp. Neurol.* **509**, 259–270. (doi:10.1002/cne.21744)
41. Lemere CA, Oh J, Stanish HA, Peng Y, Pepivani I, Fagan AM, Yamaguchi H, Westmoreland SV, Mansfield KG. 2008 Cerebral amyloid-beta protein accumulation with aging in cotton-top tamarins: a model of early Alzheimer's disease? *Rejuvenation Res.* **11**, 321–332. (doi:10.1089/rej.2008.0677)
42. Mestre-Francés N, Keller E, Calenda A, Barelli H, Checler F, Bons N. 2000 Immunohistochemical analysis of cerebral cortical and vascular lesions in the primate *Microcebus murinus* reveal distinct amyloid β1–42 and β1–40 immunoreactivity profiles. *Neurobiol. Dis.* **7**, 1–8. (doi:10.1006/nbdi.1999.0270)
43. Kraska A *et al.* 2011 Age-associated cerebral atrophy in mouse lemur primates. *Neurobiol. Aging* **32**, 894–906. (doi:10.1016/j.neurobiolaging.2009.05.018)
44. Sloane JA, Pietropaolo MF, Rosene DL, Moss MB, Peters A, Kemper T, Abraham CR. 1997 Lack of correlation between plaque burden and cognition in the aged monkey. *Acta Neuropathol.* **94**, 471–478. (doi:10.1007/s004010050735)
45. Latimer CS *et al.* 2019 A nonhuman primate model of early Alzheimer's disease pathologic change: implications for disease pathogenesis. *Alzheimer's Dementia* **15**, 93–105. (doi:10.1016/j.jalz.2018.06.3057)
46. Rodriguez-Callejas JD, Fuchs E, Perez-Cruz C, Perez-Cruz C. 2016 Evidence of tau hyperphosphorylation and dystrophic microglia in the common marmoset. *Front. Aging Neurosci.* **8**, 1–15. (doi:10.3389/fnagi.2016.00315)
47. Delacourte A, Sautiere PE, Wattez A, Mourton-Gilles C, Petter A, Bons N. 1995 Biochemical characterization of Tau proteins during cerebral aging of the lemurian primate *Microcebus murinus*. *C. R. Acad. Sci. III* **318**, 85–89.
48. Elfenbein HA, Rosen RF, Stephens SL, Switzer RC, Smith Y, Pare J, Mehta PD, Warzok R, Walker LC. 2007 Cerebral beta-amyloid angiopathy in aged squirrel monkeys. *Histol. Histopathol.* **22**, 155–167. (doi:10.14670/HH-22.155)
49. Schultz C, Hubbard GB, Rüb U, Braak E, Braak H. 2000 Age-related progression of tau pathology in brains of baboons. *Neurobiol. Aging* **21**, 905–912. (doi:10.1016/S0197-4580(00)00176-7)
50. Peters A, Verderosa A, Sethaers C, Sethares C. 2008 The neuroglial population in the primary visual cortex of the aging rhesus monkey. *Glia* **56**, 1151–1161. (doi:10.1002/glia.20686)
51. Sherwood CC, Gordon AD, Allen JS, Phillips KA, Erwin JM, Hof PR, Hopkins WD. 2011 Aging of the cerebral cortex differs between humans and chimpanzees. *Proc. Natl Acad. Sci. USA* **108**, 13 029–13 034. (doi:10.1073/pnas.1016709108)
52. Lacreuse A, Herndon JG. 2009 Nonhuman primate models of cognitive aging. In *Animal models of human cognitive aging* (eds JL Bizon, AG Woods), pp. 29–58. Totowa, NJ: Humana Press.
53. Parr L, Lacreuse A, Parr L, Chennareddi L, Herndon JG. 2018 Age-related decline in cognitive flexibility in female chimpanzees. *Neurobiol. Aging* **72**, 83–88. (doi:10.1016/j.neurobiolaging.2018.08.018)
54. Herndon JG, Moss MB, Rosene DL, Killiany RJ. 1997 Patterns of cognitive decline in aged rhesus monkeys. *Behav. Brain Res.* **87**, 25–34. (doi:10.1016/S0166-4328(96)02256-5)
55. Picq J-L, Aujard F, Volk A, Dhenain M. 2012 Age-related cerebral atrophy in nonhuman primates predicts cognitive impairments. *Neurobiol. Aging* **33**, 1096–1109. (doi:10.1016/j.neurobiolaging.2010.09.009)
56. Rapp PR, Amaral DG. 1991 Recognition memory deficits in a subpopulation of aged monkeys resemble the effects of medial temporal lobe damage. *Neurobiol. Aging* **12**, 481–486. (doi:10.1016/0197-4580(91)90077-W)
57. Munger EL, Takemoto A, Raghanti MA, Nakamura K. 2017 Visual discrimination and reversal learning in aged common marmosets (*Callithrix jacchus*). *Neurosci. Res.* **124**, 57–62. (doi:10.1016/j.neures.2017.06.002)
58. Shamy JL, Habeck C, Hof PR, Amaral DG, Fong SG, Buonocore MH, Stern Y, Barnes CA, Rapp PR. 2011 Volumetric correlates of spatiotemporal working and recognition memory impairment in aged rhesus monkeys. *Cereb. Cortex* **21**, 1559–1573. (doi:10.1093/cercor/bhq210)
59. Herndon JG, Tigges J, Anderson DC, Klumpp SA, McClure HM. 1999 Brain weight throughout the life span of the chimpanzee. *J. Comp. Neurol.* **409**, 567–572. (doi:10.1002/(SICI)1096-9861(19990712)409:4<567::AID-CNE4>3.0.CO;2-J)
60. Duan H, Wearne SL, Rocher AB, Macedo A, Morrison JH, Hof PR. 2003 Age-related dendritic and spine changes in corticocortically projecting neurons in macaque monkeys. *Cereb. Cortex* **13**, 950–961. (doi:10.1093/cercor/13.9.950)
61. Cargill R, Kohama SG, Struve J, Su W, Banine F, Witkowski E, Back SA, Sherman LS. 2012 Astrocytes in aged nonhuman primate brain gray matter synthesize excess hyaluronan. *Neurobiol. Aging* **33**, 830.e13–830.e24. (doi:10.1016/j.neurobiolaging.2011.07.006)
62. Harada N, Nishiyama S, Satoh K, Fukumoto D, Kakiuchi T, Tsukada H. 2002 Age-related changes in the striatal dopaminergic system in the living brain: a multiparametric PET study in conscious monkeys. *Synapse* **45**, 38–45. (doi:10.1002/syn.10082)
63. Coskren PJ, Luebke JI, Kabaso D, Wearne SL, Yadav A, Rumbell T, Hof PR, Weaver CM. 2015 Functional consequences of age-related morphologic changes to pyramidal neurons of the rhesus monkey prefrontal cortex. *J. Comp. Neurosci.* **38**, 263–283. (doi:10.1007/s10827-014-0541-5)
64. Erwin JM, Nimchinsky EA, Gannon PJ, Perl DP, Hof PR. 2001 The study of brain aging in great apes. In *Functional neurobiology of aging*, pp. 447–455. San Diego, CA: Academic Press. See https://www.sciencedirect.com/science/article/pii/B9780123518309500317.
65. Perl DP, Good PF, Bussière T, Morrison JH, Erwin JM, Hof PR. 2000 Practical approaches to stereology in

the setting of aging- and disease-related brain banks. *J. Chem. Neuroanat.* **20**, 7–19. (doi:10.1016/S0891-0618(00)00077-6)

66. Peters A, Sethares C, Moss MB. 1998 The effects of aging on layer 1 in area 46 of prefrontal cortex in the rhesus monkey. *Cereb. Cortex* **8**, 671–678. (doi:10.1093/cercor/8.8.671)
67. Rosene DL. 1993 Comparing age-related changes in the basal forebrain and hippocampus of the rhesus monkey. *Neurobiol. Aging* **14**, 669–670. (doi:10.1016/0197-4580(93)90065-J)
68. West MJ, Amaral DJ, Rapp PR. 1993 Preserved hippocampal cell number in aged monkeys with recognition memory deficits. *Soc. Neurosci. Abstr.* **19**, 599.
69. Gazzaley AH, Thakker MM, Hof PR, Morrison JH. 1997 Preserved number of entorhinal cortex layer II neurons in aged macaque monkeys. *Neurobiol. Aging* **18**, 549–553. (doi:10.1016/S0197-4580(97)00112-7)
70. Shobin E *et al.* 2017 Microglia activation and phagocytosis: relationship with aging and cognitive impairment in the rhesus monkey. *GeroScience* **39**, 199–220. (doi:10.1007/s11357-017-9965-y)
71. Sloane JA, Hollander W, Moss MB, Rosene DL, Abraham CR. 1999 Increased microglial activation and protein nitration in white matter of the aging monkey. *Neurobiol. Aging* **20**, 395–405. (doi:10.1016/S0197-4580(99)00066-4)
72. Sheffield LG, Berman NE. 1998 Microglial expression of MHC class II increases in normal aging of nonhuman primates. *Neurobiol. Aging* **19**, 47–55. (doi:10.1016/S0197-4580(97)00168-1)
73. Haley GE, Kohama SG, Urbanski HF, Raber J. 2010 Age-related decreases in SYN levels associated with increases in MAP-2, ApoE, and GFAP levels in the rhesus macaque prefrontal cortex and hippocampus. *Age* (*Omaha*) **32**, 283–296. (doi:10.1007/s11357-010-9137-9)
74. Edler MK *et al.* 2018 Microglia changes associated to Alzheimer's disease pathology in aged chimpanzees. *J. Comp. Neurol.* **526**, 1–16. (doi:10.1002/cne.24484)
75. Munger EL *et al.* 2019 Astrocytic changes with aging and Alzheimer's disease-type pathology in chimpanzees. *J. Comp. Neurol.* **527**, 1179–1195. (doi:10.1002/cne.24610)
76. Anderton BH. 2002 Ageing of the brain. *Mech. Ageing Dev.* **123**, 811–817. (doi:10.1016/S0047-6374(01)00426-2)
77. Bakkour A, Morris JC, Wolk DA, Dickerson BC. 2013 The effects of aging and Alzheimer's disease on cerebral cortical anatomy: specificity and differential relationships with cognition. *Neuroimage* **76**, 332–344. (doi:10.1016/j.neuroimage.2013.02.059)
78. Montine TJ *et al.* 2012 National Institute on Aging-Alzheimer's association guidelines for the neuropathologic assessment of Alzheimer's disease: a practical approach. *Acta Neuropathol.* **123**, 1–11. (doi:10.1007/s00401-011-0910-3)
79. Hof PR, Morrison JH. 1994 The cellular basis of cortical disconnection in Alzheimer's disease and related dementing conditions. In *Alzheimer's disease* (eds RD Terry, R Katzman, KL Bick), pp. 197–229. New York, NY: Raven.
80. Hof PR, Morrison JH. 2004 The aging brain: morphomolecular senescence of cortical circuits. *Trends Neurosci.* **27**, 607–613. (doi:10.1016/j.tins.2004.07.013)
81. Slomianka L, West MJ. 2005 Estimators of the precision of stereological estimates: an example based on the CA1 pyramidal cell layer of rats. *Neuroscience* **136**, 757–767. (doi:10.1016/j.neuroscience.2005.06.086)
82. Sherwood CC, Raghanti MA, Wenstrup JJ. 2005 Is humanlike cytoarchitectural asymmetry present in another species with complex social vocalization? A stereologic analysis of mustached bat auditory cortex. *Brain Res.* **1045**, 164–174. (doi:10.1016/j.brainres.2005.03.023)
83. Dorph-Petersen KA, Nyengaard JR, Gundersen HJ. 2001 Tissue shrinkage and unbiased stereological estimation of particle number and size. *J. Microsc.* **204**, 232–246. (doi:10.1046/j.1365-2818.2001.00958.x)
84. Keuker JIH, Luiten PGM, Fuchs E. 2003 Preservation of hippocampal neuron numbers in aged rhesus monkeys. *Neurobiol. Aging* **24**, 157–165. (doi:10.1016/S0197-4580(02)00062-3)
85. West MJ. 1993 Regionally specific loss of neurons in the aging human hippocampus. *Neurobiol. Aging* **14**, 287–293. (doi:10.1016/0197-4580(93)90113-P)
86. Braak H, Braak E. 1991 Neuropathological stageing of Alzheimer-related changes. *Acta Neuropathol.* **82**, 239–259. (doi:10.1007/BF00308809)
87. Thal DR, Rüb U, Orantes M, Braak H. 2002 Phases of a beta-deposition in the human brain and its relevance for the development of AD. *Neurology* **58**, 1791–1800. (doi:10.1212/WNL.58.12.1791)
88. Nirzhor SSR, Khan RI, Neelotpol S. 2018 The biology of glial cells and their complex roles in Alzheimer's disease: new opportunities in therapy. *Biomolecules* **8**, 93. (doi:10.3390/biom8030093)
89. Bussière T *et al.* 2004 Morphological characterization of thioflavin-S-positive amyloid plaques in transgenic Alzheimer mice and effect of passive Aβ immunotherapy on their clearance. *Am. J. Pathol.* **165**, 987–995. (doi:10.1016/S0002-9440(10)63360-3)
90. Von Gunten A, Kövari E, Rivara CB, Bouras C, Hof PR, Giannakopoulos P. 2005 Stereologic analysis of hippocampal Alzheimer's disease pathology in the oldest-old: evidence for sparing of the entorhinal cortex and CA1 field. *Exp. Neurol.* **193**, 198–206. (doi:10.1016/j.expneurol.2004.12.005)
91. Giannakopoulos P, Herrmann FR, Bussiere T, Bouras C, Kovari E, Perl DP, Morrison JH, Gold G, Hof PR. 2003 Tangle and neuron numbers, but not amyloid load, predict cognitive status in Alzheimer's disease. *Neurology* **60**, 1495–1500. (doi:10.1212/01.WNL.0000063311.58879.01)
92. Giannakopoulos P, Kövari E, Herrmann FR, Hof PR, Bouras C. 2009 Interhemispheric distribution of Alzheimer disease and vascular pathology in brain aging. *Stroke* **40**, 983–986. (doi:10.1161/STROKEAHA.108.530337)
93. Serrano-Pozo A, Gomez-Isla T, Growdon JH, Frosch MP, Hyman BT. 2013 A phenotypic change but not proliferation underlies glial responses in Alzheimer disease. *Am. J. Pathol.* **182**, 2332–2344. (doi:10.1016/j.ajpath.2013.02.031)
94. Shah P, Lal N, Leung E, Traul DE, Gonzalo-Ruiz A, Geula C. 2010 Neuronal and axonal loss are selectively linked to fibrillar amyloid-β within plaques of the aged primate cerebral cortex. *Am. J. Pathol.* **177**, 325–333. (doi:10.2353/ajpath.2010.090937)
95. Geula C, Wu CK, Saroff D, Lorenzo A, Yuan M, Yankner BA. 1998 Aging renders the brain vulnerable to amyloid beta-protein neurotoxicity. *Nat. Med.* **4**, 827–831. (doi:10.1038/nm0798-827)
96. Forny-Germano L *et al.* 2014 Alzheimer's disease-like pathology induced by Aβ oligomers in non-human primates. *J. Neurosci.* **34**, 13 629–13 643. (doi:10.1523/JNEUROSCI.1353-14.2014)
97. Peters A, Josephson K, Vincent SL. 1991 Effects of aging on the neuroglial cells and pericytes within area 17 of the rhesus monkey cerebral cortex. *Anat. Rec.* **229**, 384–398. (doi:10.1002/ar.1092290311)
98. Bahney J, Biology C, von Bartheld CS, Bahney J, Herculano-Houzel S. 2017 The search for true numbers of neurons and glial cells in the human brain: a review of 150 years of cell counting. *J. Comp. Neurol.* **524**, 3865–3895. (doi:10.1002/cne.24040)
99. Sherwood CC *et al.* 2006 Evolution of increased glia-neuron ratios in the human frontal cortex. *Proc. Natl Acad. Sci. USA* **103**, 13 606–13 611. (doi:10.1073/pnas.0605843103)